Nchwaningite, $Mn_2^{2+}SiO_3(OH)_2 \cdot H_2O$, a new pyroxene-related chain silicate from the N'chwaning mine, Kalahari manganese field, South Africa

Daniel Nyfeler, Thomas Armbruster

Laboratorium für chemische und mineralogische Kristallographie, Universität Bern, Freiestrasse 3, CH-3012 Bern, Switzerland

Roger Dixon

Museum of the Geological Survey, PB X112, 0001 Pretoria, South Africa

Vladimir Bermanec

Department of Mineralogy and Petrology of Faculty of Science, University of Zagreb, Demetrova 1, 41000 Zagreb, Croatia

Abstract

Nchwaningite, $Mn_2^{2+}SiO_3(OH)_2 \cdot H_2O$, is an orthorhombic chain silicate [space group $Pca2_1$, $Z = 4$, $a = 12.672(9)$, $b = 7.217(3)$, $c = 5.341(2)$ Å], occurring as aggregates shaped like pin cushions, together with calcite, bultfonteinite, and chlorite at N'chwaning mine, located in the Kalahari manganese field, northern Cape Province, South Africa. The aggregates consist of light brown, transparent needles, which average $1.0 \times 0.1 \times 0.05$ mm in size. Nchwaningite is named after the mine N'chwaning II, where it was found first. Nchwaningite is biaxially negative with the refractive indices $\alpha = 1.681(2)$, $\beta = 1.688(2)$, $\gamma = 1.690(2)$, $2V_x = 54.4(4)°$. The optical orientation is $X = \mathbf{b}$, $Y = \mathbf{a}$, $Z = \mathbf{c}$. Nchwaningite has two perfect cleavages parallel to (010) and (100). The calculated density is 3.202 g/cm³. The chemical composition, as determined by electron microprobe analyses, indicates minor substitutions of Mg for Mn.

The crystal structure, including H positions, was solved and refined from X-ray single-crystal data to $R = 2.14\%$, $R_w = 2.91\%$. The nchwaningite structure consists of double layers of laterally linked so-called truncated pyroxene-building units formed by a double chain of octahedra, topped with a *Zweier* single chain of Si tetrahedra. Symmetry-equivalent units are linked laterally but turned upside down. This yields a double-layer structure with H bridges linking the layers. A striking feature of the structure is that one MnO_6 corner is formed by a H_2O molecule.

The tetrahedral chain and octahedral distortion of the new mineral is compared with pyroxenes having Mn^{2+} in M1 [synthetic $MnSiO_3$ ($P2_1/c$ clinopyroxene) and johannsenite $CaMn(SiO_3)_2$]. To test a complete Ca and Mg substitution for Mn in the new nchwaningite structure type, distance least-square refinements were performed. It was found that Ca and Mg analogues would also yield reasonable interatomic distances and polyhedra.

Occurrence and origin

The Kalahari manganese field is the largest continental Mn deposit on the Earth, located in the northern Cape Province, South Africa. Three Mn layers are interbedded with Fe formations of the Hotazel Formation of the Transvaal Sequence. These layers cover an area of about 35×15 km, and the ore varies in thickness from 6 to 45 m, with reserves of about 1.3 billion tons (Taljaardt, 1982).

Several controversial theories about the primary sedimentary origin of the Mn ores exist: Beukes (1983) and Nel et al. (1986) postulated a volcanogenic or volcano-exhalative source for Fe and Mn, related with submarine volcanism in a basin west of the Kapvaal craton. The precipitation of Fe and Mn resulted from an upwelling of O_2-undersaturated, Fe- and Mn-rich bottom waters on the shelf in a photic zone with the first O_2 producers. The

sedimentation of the distinct Fe and Mn formations resulted from the different conditions of solubility and precipitation of Fe and Mn, related to cyclic sea-level changes. Furthermore, Beukes and Gutzmer (personal communication) assumed a primary precipitation of braunite together with calcium manganese carbonates, whereas Bau (personal communication), using REE-data, postulated a primary Mn^{2+} precipitate with braunite as a secondary product. Using trace-element profiles in the Ongeluk lavas, Schuette and Cornell (1992) postulated an early alteration of fresh andesites caused by heated sea water, leading to the precipitation of Fe and Mn.

The majority of the ore, the so-called Mamatwan type, is a fine crystalline sedimentary laminated braunite and kutnohorite lutite of relatively low grade, containing a maximum of ~38 wt% Mn. A small portion of the ore is developed as coarse crystalline massive Wessels-type ore of relatively high grade with Mn contents between 42

TABLE 1. Chemical analysis of nchwaningite

	1	2	3	4	5	Av.
SiO_2	27.54	29.65	26.12	29.43	27.34	28.02
Al_2O_3	0.25	0.32	0.23	0.32	0.25	0.27
FeO	0.32	0.16	0.37	0.16	0.32	0.27
MnO	62.62	59.41	56.95	58.97	62.17	60.02
MgO	1.45	2.26	2.26	2.24	1.44	1.93
CaO	0.25	0.15	0.15	0.15	0.25	0.19
Formula normalized on (Si + Al + Fe + Mn + Mg + Ca) = 3						
Si	0.989	1.059	0.999	1.059	0.998	1.021
Al	0.011	0.013	0.010	0.014	0.011	0.012
Fe	0.010	0.005	0.012	0.005	0.010	0.008
Mn	1.904	1.797	1.844	1.797	1.904	1.849
Mg	0.078	0.120	0.129	0.120	0.078	0.105
Ca	0.010	0.006	0.006	0.006	0.010	0.008
Σ charges	7.993	8.131	8.008	8.134	8.029	8.059

Note: oxides are given as weight percents.

and 48 wt%. Wessels-type ore is restricted to the faulted northwestern part of the Mn fields in the vicinity of N'chwaning and Wessels mines (Nel et al., 1986, and references therein). Wessels-type ore is composed of hausmannite, bixbyite, braunite II, manganite, and gangue minerals such as gaudefroyite, hydrous calcium manganese silicates, andradite, etc. (Dixon, 1989; Gutzmer and Beukes, 1993). Gutzmer and Beukes (1993, and references therein) postulate that Wessels-type ore resulted from the hydrothermal upgrade of sedimentary Mamatwan-type ore precursors.

Nchwaningite itself was found in one vug in N'chwaning mine and in another vug in Wessels mine (von Bezing, personal communication). Both vugs are sited in the same stratigraphic layer, and both are related to late fault zones. Along these faults a Fe- and Si-oversaturated fluid penetrated on a small scale the Mn ore, yielding a zone of intense hematitization a few meters thick. The temperature is estimated to be in a range of 270–420 °C, with pressures between 0.2–1.0 kbar (Gutzmer and Beukes, 1993). Nchwaningite occurs as small radiating balls, up to 5 mm in diameter, of acicular crystals. It overgrows calcite and occurs with bultfonteinite and chlorite.

This new mineral has been approved by the I.M.A. Commission on New Minerals and Mineral Names. The holotype of the investigated material is deposited in the Museum of the Geological Survey in Pretoria (South Africa) under catalogue number MGS 28362, and in the Naturhistorisches Museum, Bernastrasse 15, CH-3005 Bern (Switzerland) under number NMB-B 8735.

EXPERIMENTAL PROCEDURE

Physical properties and chemical composition

The crystal habit was measured and the forms were identified on a CAD4 single-crystal X-ray diffractometer equipped with binoculars. A polarizing microscope equipped with a spindle stage was used for the determination of the optical properties. The positions of the principal vibration directions X, Y, and Z and the optic axial angle were calculated from extinction measurements using the program EXCALIBR II (Bartelmehs et al., 1992).

Refractive indices were measured by the immersion method with white light, using the Becke line method.

The chemical composition (Table 1) was determined on a JEOL JXA 50A electron microprobe at 15 kV and with a beam current of 0.255 μA. Standards used were pyrolusite for Mn, corundum for Al, periclase for Mg, hematite for Fe, wollastonite for Ca and Si, albite for Na, orthoclase for K, and celestine for Sr. The H_2O content was determined by single-crystal structure refinement.

Crystal-structure and X-ray powder data

Single-crystal X-ray data of a nchwaningite crystal 0.97 × 0.17 × 0.07 mm in size were measured on a CAD4 single-crystal diffractometer with graphite monochromatized MoKα radiation up to $\theta = 30°$ in a 3° ω-scan mode. Out of 1596 reflections, 1341 were unique and had $I > 3\sigma_I$. Cell dimensions were refined on the basis of 22 reflections with $17° > \theta > 11°$ in an orthogonal system yielding $a = 12.672(9)$, $b = 7.217(3)$, and $c = 5.341(2)$ Å. Data reduction was carried out using the SDP program library (Enraf-Nonius, 1983). The structure was solved by direct methods with the program SHELXTL (Siemens, 1990) in the space group $Pca2_1$, where the z coordinate of M1 has been fixed at 0 in order to define the origin in the acentric space group. The same program was used for structure refinement (weighted $1/\sigma^2$). H atoms were located on difference-Fourier maps and also refined. The refinement converged to $R = 2.14$, $R_w = 2.91\%$, with 96 parameters, including anisotropic displacement parameters, for all atoms except H. In addition, the Mn and Mg populations on M1 and M2 were allowed to vary. The largest residual peaks in the difference-Fourier map were 0.9 e/Å³, close to M1 and M2. Observed and calculated structure factors are given in Table 2.[1]

The atomic positions and displacement parameters from the structure refinement were used to calculate an X-ray diffraction pattern using the program Lazy Pulverix (Yvon et al., 1977). An X-ray powder diffraction pattern was recorded with a Guinier camera at room temperature using FeKα₁ radiation. Intensities were estimated by eye. The indexing of the observed pattern was based on these calculated diffraction data. Unit cell dimensions from the powder pattern were refined with the program Gitter (Hummel, 1988).

RESULTS

Morphology

Nchwaningite occurs as brown radiating balls of acicular crystals. The largest crystals are about 1.0 × 0.2 × 0.1 mm. The crystals form pointed needles elongated parallel to the crystallographic c axis (Fig. 1). The needles are platy parallel to (010) and terminated by subordinate

---

[1] A copy of Table 2 may be ordered as Document AM-95-583 from the Business Office, Mineralogical Society of America, 1130 Seventeenth Street NW, Suite 330, Washington, DC 20036, U.S.A. Please remit $5.00 in advance for the microfiche.
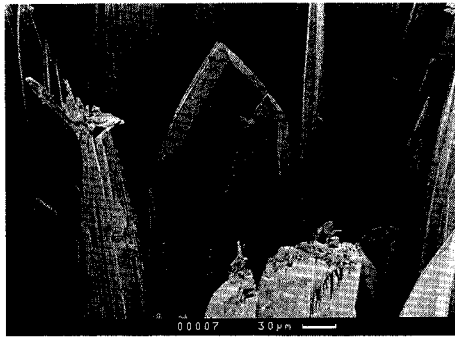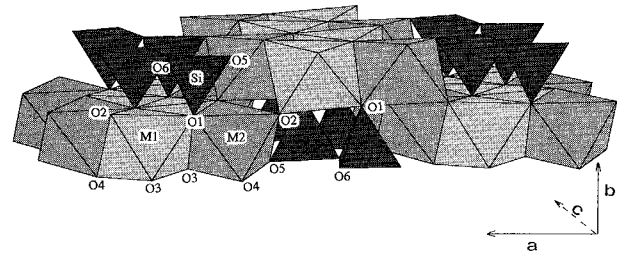
Fig. 1. SEM image of nchwaningite crystals.

Fig. 2. Layer unit of the nchwaningite structure without H atoms. SiO_4 tetrahedra are shown in dark shading. Note the different shading of the two octahedra.

(110) faces. The point is formed by faces of the type ($h0l$), predominantly (201) and (301).

Physical and optical properties

Nchwaningite is light brown and transparent with two perfect cleavages parallel to the long axis of the crystal (c axis), i.e., parallel to (100) and (010). The streak is white; the luster is vitreous. It is inert under short- and longwave UV light. The calculated density is 3.202 g/cm³. Because of the scarcity of sample material, the density was not measured. Nchwaningite has refractive indices α = 1.681(2), β = 1.688(2), γ = 1.690(2)°. The optical orientation is Y = a, X = b, Z = c. The new mineral is optically biaxial negative, with Δ = 0.009(2) calculated from refractive indices. The optical axial angle was measured to be $2V_x$ = 54.4(4)° and calculated from refractive indices to be $2V_x$ = 56.0°. Calculation of the Gladstone-Dale relationship yielded a compatibility $(1 - K_p/K_c)$ of 0.0324 (Mandarino, 1976, 1979), which is considered to be in excellent agreement.

Chemical composition

Results of the chemical analysis are given in Table 1. The following average chemical formula (based on Si + Al + Fe + Mn + Mg + Ca = 3) was derived for the new mineral: $(Mn_{1.849}Mg_{0.105}Fe_{0.008}Ca_{0.008}Al_{0.012})Si_{1.021}O_3(OH)_2 \cdot$

H_2O. The structure refinement yielded four H atoms. The original analysis gave less H_2O (by weight difference) because of loss of H_2O caused by the vacuum in the microprobe. The valence of Mn (2+) was determined from the characteristic coordination obtained by crystal structure refinement.

Crystal structure

Atomic coordinates and anisotropic displacement parameters are given in Table 3. The structure of nchwaningite consists of a tetrahedral *Zweier* single chain with O6 as bridging and O1 and O5 as nonbridging atoms (Fig. 2). These chains run parallel to the c axis and are linked by O1 to a parallel underlying double chain of Mn octahedra (M1, M2). This double chain of octahedra topped with the *Zweier* single chain forms the building unit both in nchwaningite and in proper pyroxenes. This fragment is therefore called the truncated pyroxene-building unit. Symmetry-equivalent units are linked laterally but turned upside down (Fig. 2), yielding a double-layer structure with H atoms linking the layers (Fig. 3). M1 shares five octahedral edges with octahedra M1 and M2, whereas M2 shares only two edges with octahedra M1 and M2. The double chains of both M1 and M2 octahedra are connected by O2 atoms. Of the six O atoms around both M sites, three are OH groups and one is a H_2O molecule. Average M-O distances are 2.177 and 2.212 Å for M1 and M2, respectively. The shorter value for M1 is in

TABLE 3. Final atomic positions and anisotropic displacement parameters for nchwaningite

Atom	x/a	y/b	z/c	U_{eq}	U_{11}	U_{22}	U_{33}	U_{23}	U_{13}	U_{12}
Mn1	0.18811(3)	0.82325(7)	0	0.0100(1)	0.0111(2)	0.0113(2)	0.077(2)	0.0010(2)	0.0003(2)	0.0002(1)
Mn2	0.95789(3)	0.16870(6)	−0.0220(1)	0.0103(1)	0.0108(2)	0.0118(2)	0.0084(2)	−0.0001(2)	−0.0005(2)	0.0014(1)
Si	0.81410(6)	−0.2139(1)	0.1877(2)	0.0082(2)	0.0089(3)	0.0078(3)	0.0078(3)	−0.0002(3)	0.0001(3)	0.0003(2)
O1	0.8171(2)	0.0097(3)	0.1733(4)	0.0100(5)	0.0131(8)	0.0079(8)	0.0090(2)	−0.0004(7)	−0.0004(6)	0.0005(6)
O2	0.9258(2)	−0.0159(3)	−0.3282(5)	0.0119(5)	0.0117(9)	0.0119(9)	0.0123(9)	0.0011(7)	−0.0006(7)	0.0003(7)
O3	0.6787(2)	0.3178(3)	0.3443(5)	0.0122(6)	0.0159(9)	0.008(1)	0.0127(9)	−0.0005(7)	0.0006(6)	−0.0019(7)
O4	0.9459(2)	0.3418(4)	0.3336(5)	0.0144(5)	0.0171(9)	0.0130(9)	0.013(1)	−0.0008(7)	−0.0036(8)	0.0006(7)
O5	0.9273(2)	−0.3084(3)	0.2310(5)	0.0117(5)	0.0104(8)	0.0116(9)	0.0132(9)	0.0003(7)	−0.0009(7)	0.0013(7)
O6	0.7677(2)	−0.2847(3)	−0.0889(4)	0.0113(5)	0.0153(9)	0.0106(8)	0.0080(8)	−0.0016(6)	−0.0021(6)	0.0013(7)
H2*	0.881(4)	−0.109(6)	0.75(1)	0.02						
H3*	0.681(3)	0.452(7)	0.355(9)	0.02						
H4*	0.936(3)	0.472(7)	0.296(9)	0.02						
H41*	0.996(4)	0.338(7)	0.47(1)	0.02						

* Positions of H atoms result from the structure refinement with O-H bonds constrained to a distance of 0.97 Å. Note that H atoms were refined with fixed isotropic displacement parameters.
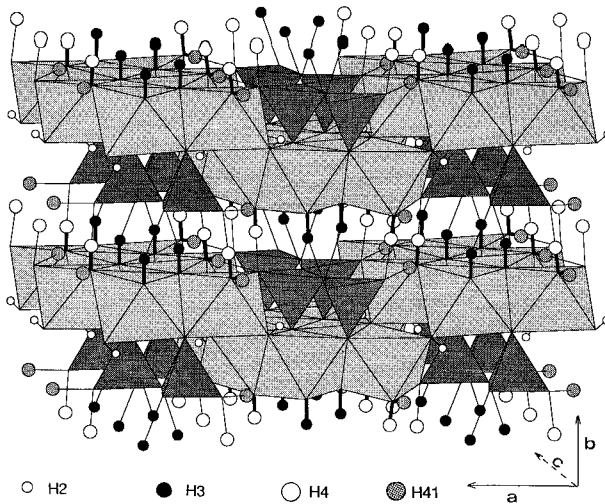
Fig. 3.   Linkage of the nchwaningite layers by H bridges. SiO₄ tetrahedra and MO₆ octahedra are shown by dark and light shading, respectively. H atoms are shown as ball and sticks. O-H bonds are thick and O···H bridges are thin.

agreement with the occupation of this site (0.86 Mn^{2+}, 0.14 Mg), whereas M2 has 0.96 Mn^{2+} and 0.04 Mg, respectively.

The maximum differences within the six M-O bonds are 0.152 Å for M1 and 0.252 Å for M2 (Table 4). However, the two longest and the two shortest bonds are not on opposite O atoms; thus no simple stretching or shortening of the octahedra, as in the case of a classical Jahn-Teller distortion, is observed. In addition, atomic displacement parameters (Table 3) of O and Mn are low and fairly isotropic; thus a dynamic Jahn-Teller effect can also be excluded. This and the characteristic Mn-O bond lengths discussed above clearly indicate the bivalent character of Mn.

The original structure refinement yielded H3 and H4 bonded to O3 and O4, with distances of 0.83 and 0.96 Å, respectively. As shown in Figure 3, these H atoms link the double layers of the nchwaningite structure. H2 is bonded to O2 with a distance of 0.59 Å, and O4 bonds an additional H atom, H41, 0.57 Å away. Note that an

TABLE 4.   Selected bond lengths (Å) and edges (Å) for nchwaningite

Mn1-O1B	2.232(2)	O3-O3	3.224(4)
Mn1-O2A	2.204(2)	O3-O2	2.899(3)
Mn1-O3A	2.139(2)	O3-O1	2.976(3)
Mn1-O3B	2.105(3)	O3-O4	3.156(4)
Mn1-O4B	2.257(3)	O1-O3	2.976(3)
Mn1-O1A	2.122(2)	O1-O2	3.003(3)
		O1-O1	3.166(3)
		O1-O4	3.023(4)
		O3-O1	2.835(4)
		O3-O4	3.391(3)
		O2-O1	3.084(3)
		O2-O4	3.161(4)
Mn2-O1	2.364(2)	O2-O2	3.274(3)
Mn2-O2	2.112(2)	O2-O5	3.162(3)
Mn2-O3C	2.160(2)	O2-O4	2.987(4)
Mn2-O4A	2.278(3)	O2-O1	3.258(4)
Mn2-O5B	2.208(2)	O2-O3	2.899(3)
Mn2-O2B	2.148(3)	O2-O5	3.007(3)
		O2-O1	3.018(3)
		O3-O5	3.243(3)
		O3-O4	3.058(4)
		O3-O1	2.835(4)
		O5-O4	3.605(4)
		O4-O1	3.023(3)
Si-O1	1.616(3)	O5-O1	2.705(3)
Si-O6	1.671(3)	O5-O6	2.657(3)
Si-O5	1.605(2)	O5-O6	2.653(3)
Si-O6A	1.661(2)	O1-O6	2.698(3)
		O1-O6	2.621(3)
		O6-O6	2.708(3)
H3···O6	2.03(5)		
H2···O6	2.10(5)		
H2···O1	2.56(6)		
H4···O5	1.63(5)		
H41···O5	1.71(6)		

Note: following Ceccarelli et al. (1981), O-H bonds were constrained to a physically reasonable 0.97 Å.

ideal O-H bond length is approximately 0.97 Å (Ceccarelli et al., 1981). This distance can be derived from X-ray diffraction data only if strong H bridges exist. Therefore, a crystal-structure refinement was also performed with O-H distances constrained to a physically reasonable 0.97 Å, following Ceccarelli et al. (1981). The resulting H positions and O···H bridging distances are added in Table 3 and Table 4, respectively. The following calculations and discussions are based on O-H bond lengths constrained to 0.97 Å. H3 forms an O···H bridge to O6 of 2.03 Å, and H4 is bridged to O5 at a distance of 1.63 Å.

TABLE 5.   Bond valences and valence sums of cations and anions in nchwaningite

	O1	O2	O3	O4	O5	O6	Σ
M1	0.395	0.315	0.378	0.275			
	0.292		0.413				2.068
M2	0.210	0.417	0.365	0.265	0.321		
		0.378					1.956
Si	1.025				1.053	0.883	
						0.905	3.866
Σ (excluding H)	1.922	1.110	1.156	0.540	1.374	1.788	
H2	0.013	0.947				0.045	1.005
H3			0.947			0.054	1.001
H4				0.947	0.159		1.106
H41				0.947	0.128		1.075
Σ (including H)	1.935	2.057	2.103	2.434	1.661	1.887	

Note: bond valences for M sites calculated taking into account their occupancy with Mn and Mg, respectively.

O4 bonds two H atoms (H4 and H41) with an angle of 106(4)° and is obviously a H_2O molecule. H41 forms a H bridge (1.71 Å) to O5 within the same double-layer unit. No well-defined H bridges could be found for H2 because $H \cdots Mn$ distances of 2.4 Å are shorter than the next $O \cdots H$ distances.

Bond valences (Brown and Altermatt, 1985) were calculated for all atoms using the constants of Brese and O'Keeffe (1991). The substitution of Mg in the M sites was considered in the calculation of the valence sums. Valence sums are compiled in Table 5. The O4 valence sum (excluding H atoms) yielded 0.540, thus representing the H_2O molecule. The sums for O2 (1.110) and O3 (1.156) both represent OH groups. The valence sum for O5 (1.375) is significantly lower than the one for O6 (1.788). This can be explained as O5 accepting two strong H bridges from H4 and H41. O6 forms H bonds to H3 and H2. The valence of O1 is 1.922, which is characteristic for O^{2-} without short H bonds. Valence sums for cations are in good agreement with their corresponding ionic charge.

X-ray powder-diffraction pattern

The powder pattern is given in Table 6. The difference between observed and calculated intensities is probably caused by preferred orientation. It is a characteristic feature of Guinier geometry that reflections of planes with preferred orientation show decreased intensity. Unit cell dimensions calculated from the indexed pattern are also given in Table 6.

DISCUSSION

Several single-chain silicates containing Mn as a major constituent are known, namely rhodonite, pyroxmangite, and bustamite. In contrast to nchwaningite, the periodicity of their single chains is 5, 7, and 3, respectively. Thus, they belong to the pyroxenoids, and we decline to compare their structures further.

The investigated mineral shows a strong structural relationship to pyroxenes. When one focuses on its similarities and differences with proper pyroxenes, the connectivity of the pyroxene-building units is noteworthy: in nchwaningite, the units within a double layer are linked by two O atoms (O2 and O5). O2 forms a common corner of the octahedra around M1 and M2 in one unit and an additional corner of M2 in the other unit (turned upside down). O5, however, links only a tetrahedral corner in one unit to a corner of the M2 octahedron in the other unit. In proper pyroxenes, the O atom corresponding to O5 in nchwaningite forms in addition a corner of the M2 polyhedron; i.e., this tetrahedral corner is linked to two octahedra. (M2 is assumed to show sixfold coordination; i.e., just octahedra are considered as possible polyhedra around M2. Note that this assumption contradicts many of the known pyroxene structures.) Furthermore, in pyroxenes, the so-called bridging O atom (the one linking the tetrahedra within the Zweier single chain) forms an additional corner of the M2 polyhedron, whereas in

TABLE 6. X-ray powder diffraction pattern of nchwaningite

I_{meas}	I_{calc}	d_{meas}	d_{calc}*	hkl
60	100	7.220	7.217	010
20	8	6.356	6.336	200
60	10	4.083	4.083	201
40	18	4.065	4.066	111
20	9	3.646	3.646	310
40	43	3.612	3.609	020
20	7	3.477	3.471	120
20	2	3.174	3.168	400
20	4	3.133	3.136	220
100	70	3.011	3.011	311
40	10	2.911	2.910	121
40	7	2.725	2.725	401
20	4	2.704	2.704	221
20	2	2.670	2.671	002
80	32	2.547	2.549	411
60	10	2.503	2.505	012
80	28	2.456	2.457	112
80	36	2.440	2.441	321
<5	2	2.381	2.381	420
<5	2	2.363	2.364	130
20	2	2.328	2.329	212
40	9	2.183	2.183	511
40	11	2.177	2.175	421
60	5	2.154	2.154	312
40	7	2.145	2.147	022
60	14	2.116	2.116	122
<5	2	2.073	2.074	520
40	4	2.041	2.042	402
<5	<1	2.030	2.033	222 / 610
20	23	1.964	1.964	601
<5	3	1.946	1.947	331
<5	4	1.935	1.933	521
20	<1	1.910	1.916	430
20	<1	1.910	1.914	322
60	35	1.804	1.803	431
40	17	1.787	1.787	032
20	8	1.759	1.756	710
60	4	1.713	1.713	113 / 203
<5	<1	1.666	1.668	213
<5	1	1.621	1.618	720
60	7	1.600	1.600	313
60	15	1.585	1.585	341 / 800
80	25	1.552	1.552	403
40	7	1.517	1.517	413
20	8	1.505	1.504	441
<5	4	1.493	1.495	042
<5	2	1.493	1.494	323
20	10	1.484	1.485	142
60	20	1.466	1.467	712

* Calculated from cell parameters refined from X-ray powder diffraction data: $a = 12.682(4)$, $b = 7.214(2)$, $c = 5.337(1)$ Å.

nchwaningite this bridging atom, O6, has only a H bridge (H3) to O3. As a consequence of these different connectivities, pyroxenes have the well-known I beams (Papike et al., 1973), whereas in nchwaningite only a truncated pyroxene building unit exists. Another major difference is the presence of both OH molecules and H_2O in nchwaningite.

Only two manganese pyroxenes with Mn^{2+} in M1 are described in the literature: johannsenite, $CaMnSi_2O_6$ (Freed and Peacor, 1967), the Mn equivalent of diopside, and a synthetic pyroxene type, $MnSiO_3$ (Tokonami et al., 1979). These two phases and nchwaningite all have a common unit in their structure: a Zweier single chain of

TABLE 7. Comparison of structures containing the truncated pyroxene-building-unit

	S-rotated				O-rotated			
	Nchwaningite		MnSiO$_3$ (pyroxene)		MnSiO$_3$ (pyroxene)		Johannsenite	
Bond lengths around Si (Å)	Si-O6	1.661	Si1-O3a	1.648	Si2-O3b	1.665	Si-O3	1.681
	Si-O6	1.671	Si1-O3a	1.666	Si2-O3b	1.670	Si-O3	1.695
	Si-O1	1.616	Si1-O1a	1.614	Si2-O1b	1.616	Si-O1	1.605
	Si-O5	1.605	Si1-O2a	1.602	Si2-O2b	1.598	Si-O2	1.595
Av. Si-O bond (Å)		1.638		1.633		1.637		1.644
Bond lengths around M1 (Å)	Mn1-O3	2.105	Mn1-O2a	2.114	Mn1-O2a	2.114	Mn-O2	2.133
	Mn1-O1	2.122	Mn1-O2b	2.131	Mn1-O2b	2.131	Mn-O2	2.133
	Mn1-O3	2.139	Mn1-O1a	2.133	Mn1-O1a	2.133	Mn-O1	2.159
	Mn1-O2	2.204	Mn1-O1b	2.157	Mn1-O1b	2.157	Mn-O1	2.159
	Mn1-O1	2.232	Mn1-O1a	2.255	Mn1-O1a	2.255	Mn-O1	2.230
	Mn1-O4	2.257	Mn1-O1b	2.274	Mn1-O1b	2.274	Mn-O1	2.230
Av. M1-O bond (Å)		2.177		2.177		2.177		2.174
Bond lengths around M2 (Å)	Mn2-O2	2.112	Mn2-O2b	2.054	Mn2-O2b	2.054	Ca-O2	2.320
	Mn2-O2	2.148	Mn2-O2a	2.088	Mn2-O2a	2.088	Ca-O2	2.320
	Mn2-O3	2.160	Mn2-O1b	2.162	Mn2-O1b	2.162	Ca-O1	2.383
	Mn2-O5	2.208	Mn2-O1a	2.180	Mn2-O1a	2.180	Ca-O1	2.383
	Mn2-O4	2.278	Mn2-O3a	2.472	Mn2-O3a	2.472	Ca-O3	2.653
	Mn2-O1	2.364	Mn2-O3b	2.732	Mn2-O3b	2.732	Ca-O3	2.653
							Ca-O3	2.769
							Ca-O3	2.769
Av. M2-O bond (Å)		2.212		2.281		2.281		2.531
Angle of O$_{br}$ atoms in tet. chain (°)	O6-O6-O6	160.9	O3a-O3a-O3a	169.5	O3b-O3b-O3b	149.5	O3-O3-O3	163.8
Angle Si-O$_{br}$-Si (°)	Si-O6-Si	139.540	Si1-O3a-Si1	139.360	Si2-O3b-Si2	134.720	Si-O3-Si	136.360
Distance Si-Si (Å)		3.126		3.108		3.078		3.134
c-cell dimension (Å)		5.341		5.298		5.298		5.293
Edge lengths of O$_{br}$ (Å)	O6-O6	2.708	O3a-O3a	2.660	O3b-O3b	2.746	O3-O3	2.673
Angle O$_{br}$-Si-O$_{br}$ (°)	O6-Si-O6	108.8	O3a-Si1-O3a	106.8	O3b-Si2-O3b	110.8	O3-Si-O3	104.7

Si tetrahedra linked to an underlying parallel double chain of octahedra (M1, M2). As mentioned above, this is called the truncated pyroxene-building unit. This unit is shown in Figure 3 for the three structures. In pyroxenes, the volume of the M2 polyhedron is at least as large as that of M1. Thus, if two M cations are available, the one with the larger ionic radius prefers the M2 site. This feature is observed for johannsenite, where the larger Ca occupies the M2 polyhedron. Furthermore, the increased size of the cation forces an eightfold coordination around M2. The MnSiO$_3$ (pyroxene) structure is similar to that of ferrosilite, both crystallizing in space group $P2_1/c$ (Cameron and Papike, 1980, noted that ferrosilite possesses various polymorphs with different space groups). MnSiO$_3$ (pyroxene) has not yet been observed in nature, but it was synthesized at 10 GPa and 1200 °C (Tokonami et al., 1979). These conditions lead to a strongly distorted M2 polyhedron and a regular M1 octahedron, both occupied by Mn^{2+}. Tokonami et al. (1979) assumed a sevenfold coordination of M2 with one long M2-O distance of 3.03 Å. However, there is also an Si-M2 distance of 2.916 Å. Thus, we assume a distorted octahedral coordination for M2 in MnSiO$_3$ (pyroxene). The M1 octahedron is similar in the three structures. Differences in average bond lengths and variations within the individual bonds are negligible. However, differences are observed in M2: a rather undeformed M2 octahedron was found for nchwaningite, whereas the polyhedron around M2 in MnSiO$_3$ (pyroxene) is strongly distorted, but still sixfold coordinated (Table 7). Although the average Si-O distance in johannsenite is slightly longer, the average Si-O

bond in the three phases remains virtually unaffected by the different sizes of the M2 site.

The interpolyhedral distortion of a *Zweier* single chain can be described following the nomenclature of Thompson (1970): a Si tetrahedral chain that is not completely extended shows an internal rotation; i.e., the angle of the O atoms linking the tetrahedra (the so-called bridging O atoms) is <180°, whereas the completely extended chain shows an angle of 180°. Depending on the orientation of the basal triangular faces of the tetrahedra, the *Zweier* single chain is either O- or S-rotated. In a S-rotated chain, the basal triangular faces of the tetrahedra have the same orientation as the triangular faces of the octahedral strip to which they are linked by the apical O atoms. In an O-rotated chain, however, these triangular faces have an orientation opposite to each other. Such an O-rotated chain is observed in johannsenite, whereas the structure of MnSiO$_3$ (pyroxene) possesses both an O-rotated and a S-rotated chain, characteristic of pyroxenes crystallized in space group $P2_1/c$. Nchwaningite possesses only one distinct S-rotated chain type.

In general, a crystal structure is constrained by chemical, electrostatic, and steric (i.e., geometric) effects. The most important electrostatic factors are expressed in terms of the individual bond valences, the valence sums of cations and anions, the repulsion of O atoms produced by intrapolyhedral distortion and the cation-cation repulsion caused by interpolyhedral distortion, and whether the chemical bond is more of an ionic or a covalent nature (Pauling, 1980). Steric effects can arise from the constraints imposed by crystal symmetry, which requires that

TABLE 8. Valence sums of cations and tetrahedron oxygens of nchwaningite, $MnSiO_3$ (pyroxene), and johannsenite

	S-rotated				O-rotated			
	Nchwaningite (incl. H)		$MnSiO_3$ (pyroxene)		$MnSiO_3$ (pyroxene)		Johannsenite	
M1		2.068	Mn1	2.137	Mn1	2.137	Mn2	2.138
M2		1.956	Mn2	1.888	Mn2	1.888	Ca	1.962
Si		3.866	Si1	3.918	Si2	3.873		3.817
O_{apical}	O1	1.935	O1a	2.057	O1a	2.057	O1	2.057
O_{br}	O6	1.887	O3a	1.988	O3b	1.856	O3	1.953
O_{M2}	O5	1.661	O2a	1.922	O2b	1.961	O2	1.863

all parts (e.g., the various coordination polyhedra) of a structure be commensurate (Brown, 1992). Each real crystal structure is the result of a complex interference of both steric and electrostatic conditions, which are hard to analyze and almost impossible to quantify. The three structures, nchwaningite, $MnSiO_3$ (pyroxene), and johannsenite, each conform to a different structural topology created by different chemical, electrostatic, and steric conditions. However, some characteristics and variations in the three structures can be discussed. The SiO_{br} bonds are consistently longer than the corresponding $Si-O_{nonbr}$ bonds. In johannsenite, for example, the two bridging O atoms are bonded to Si with distances of 1.681 and 1.695 Å, respectively. This deviation from the average (1.644 Å) is assumed to be due to a given geometric environment, i.e., the diopside-type structure of johannsenite. The $Si-O_{br}$ bonds exceed the usual average bond lengths for similar bonds in a tetrahedral chain (Liebau, 1985). The other two O atoms compensate for this deficient bond valence by shorter Si-O bonds (1.605 and 1.595 Å). According to Brese and O'Keeffe (1991) and as discussed in detail in Brown (1992), this deviation from the average bond lengths allows a sufficient valence sum for Si (3.817) in johannsenite. The long $Si-O_{br}$ distances allow a narrow $O_{br}-Si-O_{br}$ angle of 104.7°. The $O_{br}-O_{br}$ distance of 2.673 Å is close to the average value; thus it confirms that there is no extraordinary anion-anion repulsion. In $MnSiO_3$ (pyroxene) and in nchwaningite, this tendency is less obvious, and probably other mechanisms are responsible for the observed dimensions. In both the O-rotated and the S-rotated chains of $MnSiO_3$ (pyroxene) and in the S-rotated chain of nchwaningite, the Si cation has a valence sum slightly higher than the Si in johannsenite (Table 8), reflecting the lower average Si-O bond length in former chains.

From a geometrical point of view, the following dimensions should increase with the increasing size of the M sites: the angle of bridging O atoms in tetrahedral chain, the angle $Si-O_{br}-Si$, the distance Si-Si, the c-cell dimension, the edge length of O_{br}, and the angle $O_{br}-Si-O_{br}$. However, in johannsenite, with the large Ca in the M2 site, only the Si-Si distance (3.134 Å) shows a positive correlation to the size of M2, whereas the other dimensions are unaffected. The increased size of the M2 polyhedra does not apparently stretch the tetrahedral chain. This feature could be due to the stiff tetrahedral chain, which constrains the length of the c-cell dimension. In

these examples there is no simple correlation between the size of the M2 site and the length of the tetrahedral chain. As shown in Table 7 and Figure 4, the two *Zweier* single chains of $MnSiO_3$ (pyroxene) are noteworthy: the O-rotated chain yields an angle of the bridging atoms O3-O3-O3 that is 20° less than the S-rotated chain. This narrow O-O-O angle of the O-rotated chain obviously produces a shortening of the Si-Si distance and a narrow $Si-O_{br}-Si$ angle, relative to the S-rotated chain. Note that both tetrahedral chains are constrained by the length of the c-axis. The apparent shortening of the O-rotated chain is compensated for by an opening of the $O_{br}-Si-O_{br}$ angle, causing, in combination with a slightly increased $Si-O_{br}$ bond, an effective stretching of the tetrahedral O3-O3 edge length of bridging O atoms.

STRUCTURE MODELING OF Ca AND Mg ANALOGUES OF NCHWANINGITE

Because nchwaningite represents a new structure type, the question arises whether this structure is restricted to Mn^{2+} in M1 and M2. To test the geometrical flexibility of this structure type, hypothetical Ca and Mg analogues were modeled with the program DLS-76 (Baerlocher et al., 1977). It aims for achieving the bond lengths predicted by the user by a distance least-squares procedure as follows:

$$\rho = \sum_j w_j^2 (D_j^0 - D_j^{m,n})^2$$

where D_j^0 is the prescribed interatomic distance, $D_j^{m,n}$ is the calculated distance of type j between atoms m and n, and w_j is the weight ascribed to the interatomic distance. Several assumptions were made such as fixed symmetry and different weights for the bonds to simulate a realistic bond valence. In addition, all O-O distances below 3 Å were considered. We assumed a weight for the Si-O bond of 1.0, a weight for the M-O bond of 0.5, and a weight for the O-O repulsion of 0.1. This value has been exaggerated with respect to the bond valences, which can be calculated according to O'Keeffe and Brese (1992). These weight factors were derived from their corresponding bond valences, with a slightly exaggerated weight for the M-O bond to force the M octahedron to the size of the respective cation. Two types of modeling were performed: one with the length of the M-O bond decreased by 0.1 Å (relative to the corresponding bond length measured in nchwaningite) to simulate Mg both in M1 and M2 and
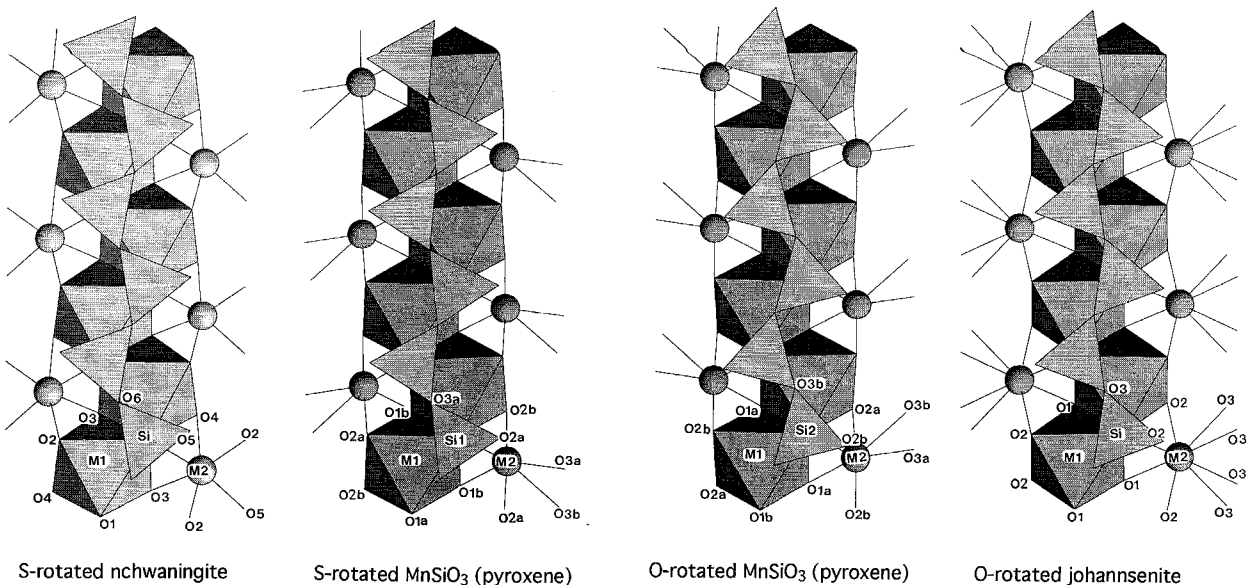
S-rotated nchwaningite   S-rotated MnSiO₃ (pyroxene)   O-rotated MnSiO₃ (pyroxene)   O-rotated johannsenite

Fig. 4. Comparison of the so-called truncated pyroxene-building units of nchwaningite, $MnSiO_3$ (pyroxene), and johannsenite. M1 and the tetrahedral chain are shown as polyhedra. M2 polyhedra are drawn with ball and sticks. In this figure, the c axis is constrained to a fixed length. The two tetrahedral chains of $MnSiO_3$ (pyroxene) have a different rotation sense.

another one with the length of the M-O bond increased by 0.18 Å to simulate Ca in the M positions. Furthermore, the a and c dimensions of the unit cell were allowed to vary, whereas the b dimension (perpendicular to the layers) was fixed. Note that for the Ca and Mg models as well as for nchwaningite itself, valence sums were calculated based on the structure refinement with O-H bonds constrained to a distance of 0.97 Å. The results of these models are listed in Tables 9 and 10. Several characteristics are compiled: the Si-O6-Si angle and the O6-O6-O6 angle describe the stretching of the tetrahedral chain. In general, the more the size of the octahedra in the underlying double chain is increased, the more the tetrahedral chain becomes stretched, yielding a wide O6-O6-O6 angle. Furthermore, the length of the c-cell dimension (parallel to the chain) is also stretched by this effect.

The edge length distortion (ELD) and bond length distortion (BLD) show the intrapolyhedral deformation, the former representing the variation in the cation-O length, the latter the variation in O-O distances forming polyhedral edges. Following Renner and Lehmann (1986), BLD and ELD are calculated as follows:

$$BLD = \frac{100}{n} \cdot \sum_{i=1}^{n} \frac{|d_i - d_m|}{d_m} \quad (\%)$$

$$ELD = \frac{100}{n} \cdot \sum_{i=1}^{n} \frac{|e_i - e_m|}{e_m} \quad (\%)$$

where n = number of cation-O bonds (BLD) or number of O-O distances (ELD), d_i = individual cation-O bond length, d_m = mean cation-O bond length, e_i = individual edge length, and e_m = mean edge length.

Interpolyhedral distortion of the tetrahedral chain

If the ionic radius in M1 and M2 is reduced from 0.83 Å (Mn^{2+}) to 0.72 Å (Mg) (Shannon, 1976), the c-cell

TABLE 9. Comparison of ELD and BLD in nchwaningite and its modeled Mg and Ca analogues

	Mg analogue	Nchwaningite	Ca analogue
R (DLS)*	0.007	n.d.	0.0115
BLD (M1)	2.670	2.504	2.066
ELD (M1)	4.430	4.098	3.464
BLD (M2)	3.929	3.296	3.205
ELD (M2)	4.489	5.200	6.245
BLD (T1)	1.694	1.694	1.694
ELD (T1)	1.606	1.122	2.246
Si-O6-Si (°)	131.29	139.54	153.85
O6-O6-O6 (°)	152.55	160.93	171.28
a dimension (Å)	12.216	12.672	13.212
c dimension (Å)	5.162	5.341	5.649

* $R = \sqrt{\Sigma_i [w_i(D_i^0 - D_i^{m,n})]^2 / \Sigma_i (wD_i^0)^2}$.

TABLE 10. Valence sums and index R1 for nchwaningite and its Ca and Mg analogues

	Mg analogue	Nchwaningite	Ca analogue
M1	2.141	2.068	2.153
M2	1.989	1.957	2.036
Si	3.866	3.866	3.866
O1	2.005	1.935	1.937
O2	2.085	2.057	2.110
O3	2.145	2.103	2.196
O4	2.428	2.434	2.471
O5	1.723	1.661	1.732
O6	1.966	1.887	1.966
Index R1	0.140	0.151	0.163

dimension (direction of the tetrahedral chain) changes to a value of 5.162 Å, which is very similar to the 5.179 Å found for $Mg_2Si_2O_6$ enstatite (Hawthorne and Ito, 1977) and to the 5.166 Å found for clinoenstatite (Ohashi and Finger, 1976). According to Cameron and Papike (1980), Si-O$_{br}$-Si angles between approximately 127 and 144° are observed in pyroxenes. Only our hypothetical Ca analogue of nchwaningite is above this range (153.85°). Given the presence of lone-pair electrons in the electron orbital of the O atom, this wide angle probably produces a certain stress. The O3-O3-O3 angle (equivalent to O6-O6-O6 in nchwaningite) in pyroxenes is between 136 and 180° (Cameron and Papike, 1980); our modeled structures (Table 9) are within this range.

Intrapolyhedral deformations

With increasing size of the M1 octahedron, both BLD and ELD decrease, indicating a more and more regular shape. BLD of M2 also decreases with increasing radius, whereas ELD increases. Therefore, the differences in ELD for M1 and M2 strongly increase with increasing M-O distance. This is caused by the relative stiffness of the *Zweier* single chain, keeping O1 (the O atom linking M1 and the tetrahedral chain) at a more or less fixed position but distorting the edges of the M2 octahedron. The edge O4-O5 is the longest in all three chemical variants but strongly stretches with increasing M-O distance.

Another interesting feature is the high ELD value for the SiO_4 tetrahedron (T1) in the Ca analogue of nchwaningite, which is mainly caused by the strongly stretched O6-O6 tetrahedral edge (2.833 Å). This stretching is apparently due to the increased M cation size. The Si-O bonds for both the Ca and Mg analogues have the same values. Thus, the whole change in the O6-O6 edge length is produced by different O6-Si-O6 angles, i.e., 116.56° for the Ca analogue, and 105.76° for the Mg analogue.

Distortion in terms of index R1

Deviations from ideal bond valences express deviations from ideal bond lengths. The higher the difference between the valence of an atom and its experimentally determined valence sum, the higher the stress imposed by the crystal structure. This discrepancy of the experimental valence sum is measured as follows:

$$d_i = V_i - \sum_j s_{ij}$$

where V_i is the cation valence and s_{ij} is the experimental bond valence between cation i and anion j. The agreement over the whole structure is expressed in the index R1 (Brown, 1992):

$$R1 = \sqrt{\langle d_i^2 \rangle}.$$

Low values of R1 imply relaxed structures, indicating a higher stability of the structure. Note that only the two cations in the M sites and Si are considered in the calculation of R1. The low value for the Mg model of nchwaningite (0.140) indicates a relaxed structure.

Nchwaningite itself shows a slightly increased index (0.151), but it is still in the same range, as is the index for the Ca model of nchwaningite, which is just slightly higher (0.163). The comparison of R1 with the BLD and ELD values produces no evidence that one of the modeled structures is unlikely to be stable. The low R1 value for the Mg model of nchwaningite suggests a relaxed structure and indicates that Mg substitution, as observed in Table 1, is favored in the nchwaningite structure type.

REFERENCES CITED

Baerlocher, Ch., Hepp, A., and Meier, W.M. (1977) DLS-76, a program for the simulation of crystal structures by geometric refinement. Eidgenössiche Technische Hochschule, Zurich.

Bartelmehs, K.L., Bloss, F.D., Downs, R.T., and Birch, J.B. (1992) EXCALIBR II. Zeitschrift für Kristallographie, 199, 185–196.

Beukes, N.J. (1983) Palaeoenvironmental setting of iron formations in the depositional basin of the Transvaal Supergroup, South Africa. In A.F. Trendall and R.C. Morris, Eds., Iron formations: Facts and problems, p. 131–209, Elsevier, Amsterdam.

Brese, N.E., and O'Keeffe, M. (1991) Bond valence parameters for solids. Acta Crystallographica, B47, 192–197.

Brown, I.D. (1992) Chemical and steric constraints in inorganic solids. Acta Crystallographica, B48, 553–572.

Brown, I.D., and Altermatt, D. (1985) Bond valence parameters obtained from a systematic analysis of the inorganic crystal structure database. Acta Crystallographica, B41, 244–247.

Cameron, M., and Papike, J.J. (1980) Crystal chemistry of silicate pyroxenes. In Mineralogical Society of America Reviews in Mineralogy, 7, 5–87.

Ceccarelli, C., Jeffrey, G.A., and Taylor, R. (1981) A survey of O-H····O hydrogen bond geometries determined by neutron diffraction. Journal of Molecular Structure, 70, 255–271.

Dixon, R.D. (1989) Sugilite and associated metamorphic silicate minerals from Wessels Mine, Kalahari manganese field. Bulletin of the Geological Survey (South Africa), 93, 1–47.

Enraf-Nonius (1983) Structure determination package (SDP), Delft, the Netherlands.

Freed, R.L., and Peacor, D.R. (1967) Refinement of the crystal structure of johannsenite. American Mineralogist, 52, 709–720.

Gutzmer, J., and Beukes, N.J. (1993) Fault zone controlled hematitization and upgrading of manganese ores in the KMF, South Africa (Conference Proceeding, Newsletter 8) IGCP Project 318: Genesis and correlation of marine polymetallic oxides, p. 139–141. Swaziland, South Africa.

Hawthorne, F.C., and Ito, J. (1977) Synthesis and crystal-structure refinement of transition-metal pyroxenes: I. Orthoenstatite and (Mg,Mn,Co) orthopyroxene. Canadian Mineralogist, 15, 321–338.

Hummel, W. (1988) Gitter, Berechnung von Gitterparametern aus Röntgen-Pulverdiagrammen, 2.0. Labor für chemische und mineralogische Kristallographie, University of Bern, Bern, Switzerland.

Liebau, F. (1985) Structural chemistry of silicates, 347 p. Springer-Verlag, Berlin.

Mandarino, J.A. (1976) The Gladstone-Dale relationship: I. Derivation of new constants. Canadian Mineralogist, 14, 498–502.

——— (1979) The Gladstone-Dale relationship: III. Some general applications. Canadian Mineralogist, 17, 71–76.

Nel, C.J., Beukes, N.J., and de Villiers, J.P.R. (1986) The Mamatwan

manganese mine of the Kalahari manganese field. In C.R. Annhaeusser and S. Maske, Eds., Mineral deposits of southern Africa, vols. 1 and 2, 963–978. Johannesburg, South Africa.

Ohashi, Y., and Finger, L.W. (1976) The effect of Ca substitution on the structure of clinoenstatite. Carnegie Institution of Washington Year Book, 75, 743–746.

O'Keeffe, M., and Brese, N.E. (1992) Bond-valence parameters for anion-anion bonds in solids. Acta Crystallographica, B48, 152–154.

Papike, J.J., Prewitt, C.T., Sueno, S., and Cameron, M. (1973) Pyroxenes: Comparisons of real and ideal structural topologies. Zeitschrift für Kristallographie, 138, 254–273.

Pauling, L. (1980) The nature of the chemical bond, 430 p. Cornell University Press, Ithaca, New York.

Renner, B., and Lehmann, G. (1986) Correlation of angular and bond length distortion in TO₄ units in crystals. Zeitschrift für Kristallographie, 175, 43–59.

Schuette, S.S., and Cornell, D.H. (1992) Extreme sea floor alteration as the source of the Kalahari manganese deposits (abs.), p. 354–356. 24th Congress of the Geological Society of South Africa, Bloemfontein, South Africa.

Shannon, R.D. (1976) Revised effective ionic radii and systematic studies of interatomic distances in halides and chalcogenides. Acta Crystallographica, A32, 751–767.

Siemens (1990) SHELXTL PC 4.1. Siemens Analytical X-ray Instruments, Madison, Wisconsin.

Taljaardt, J.J. (1982) Major manganese ore fields, SAMANCOR (South African Manganese Amcor Limited) internal report, Republic of South Africa.

Thompson, J.B., Jr. (1970) Geometrical possibilities for amphibole structures: Model biopyriboles. American Mineralogist, 55, 292–293.

Tokonami, M., Horiuchi, H., Nakano, A., Akimoto, S., and Morimoto, N. (1979) The crystal structure of the pyroxene-type $MnSiO_3$. Mineralogical Journal, 9, 424–426.

Yvon, K., Jeitschko, W., and Parthe, E. (1977) Lazy Pulverix, a computer program for calculating X-ray and neutron diffraction powder patterns. Journal of Applied Crystallography, 10, 73–74.